Practical performance limits of solar power-to-heat cascades

Eduardo González-Mora[a], Ram Poudel[b] and Ma. Dolores Durán-García[a]

[a] *Universidad Autónoma del Estado de México, Toluca, México, egonzalezmo@uaemex.mx, CA*
[b] *Appalachian State University, Boone, USA, poudelrc@appstate.edu*

Abstract:

Thermodynamics establishes the fundamental efficiency limits for converting heat into useful effects. For solar thermal systems, these principles define the maximum possible performance for applications ranging from domestic heating to industrial process heat. The theoretical maximum for delivering heat via a reversible cascade of a heat engine and heat pump—the so-called Jaynes-engine—promises significant gains but neglects the finite-rate irreversibilities inherent in real devices. Historically, the practical embodiment of this concept, the Vuilleumier cycle, demonstrated the engineering recognition of this architecture nearly a century ago. However, establishing realistic performance limits requires explicitly modelling irreversibilities in both the work-producing and work-consuming subunits. Here we develop a comprehensive non-equilibrium thermodynamic model for a solar-driven heat transformer, comprising an irreversible radiative work extractor coupled with an irreversible work consumer. By systematically incorporating external heat transfer irreversibilities and internal dissipation, we derive the endoreversible condition to isolate the fundamental performance ceiling. We show that the radiation-driven heat transformer consistently outperforms conventional radiative heating, achieving gain factors significantly greater than unity across all operational regimes. The analysis reveals a profound structural shift in parametric influence: the sensitivity to solar concentration increases five-fold compared to conventional systems, attaining near-parity with target temperature as a dominant control variable. Specifically, optical concentration accounts for 41.5 % of total parametric influence in the transformer, versus only 12.6 % in conventional configurations. These findings significantly refine and extend the foundational bounds established by previous endoreversible models, demonstrating that optical concentration assumes unprecedented importance in coupled architectures—an insight absent from earlier work that treated subsystems in isolation. By quantifying the interplay between optical quality and thermodynamic coupling, this work establishes rigorous benchmarks for next-generation solar thermal technologies, informing the rational design of systems aimed at decarbonising industrial heat—a sector accounting for nearly half of global final energy consumption.

Keywords:

Solar thermal energy; Heat transformer; Irreversibility analysis; Endoreversible thermodynamics.

1. Introduction

In contemporary energy discourse, thermal energy frequently remains a neglected dimension, often overshadowed by the high-profile transitions occurring within the electricity and transport sectors. Nevertheless, its significance within the global energy matrix is paramount. According to the latest findings from REN21, heat continues to account for 46% of total final energy consumption globally, underscoring its critical role and the urgent need for focused decarbonisation strategies in this sector [1].

Given this substantial demand, determining appropriate means for supplying heat across the various consuming sectors is critically important. Addressing this necessity requires a shift from conventional, dissipative methods towards more sophisticated thermodynamic systems. The exploration of such efficiency often begins with Lord Kelvin (William Thomson), who famously established the maximum theoretical limit for converting heat into work [2]. However, a significant yet often overlooked development is the "dual theorem" that E.T. Jaynes articulated in 2003 [3], which focuses on the maximum efficiency of converting heat at one temperature into heat at another. In a traditional heating scenario, heat simply degrades directly from a high-temperature source to a lower-temperature target—a process that is fundamentally irreversible because it generates entropy and wastes thermodynamic potential. Jaynes [3] demonstrated that conducting the process reversibly could vastly improve performance: a perfect Carnot engine extracts work from a high-temperature source, and that work subsequently powers a heat pump that draws additional thermal energy from the ambient environment.

This theoretical arrangement can achieve a heating gain factor significantly higher than unity, suggesting that buildings and industrial processes could, in principle, operate with far greater efficiency than current practice achieves. Whilst Jaynes presented this as a "little known" fact of great pedagogical interest, the underlying concept was not entirely new. Nearly a century earlier, Rudolph Vuilleumier patented a "Method and Apparatus for Inducing Heat Changes" [4]. In contrast to the generalised, theoretical treatment that Jaynes provided, Vuilleumier proposed a practical, operative machine consisting of a confined fluid moving between different temperature zones through regenerators to induce secondary heating or cooling effects. Although little historical evidence suggests that Vuilleumier constructed a large-scale commercial device [5], his patent explicitly outlined the mechanical and thermodynamic principles of what we now recognise as the Vuilleumier cycle—a heat-driven cycle that integrates a heat engine and a heat pump into a single assembly.

However, whilst Jaynes' reversible model provided an "elegant treatment", it established an unattainable upper limit by neglecting the inherent irreversibilities of real systems. To determine a realistic limit for the combination of a heat engine and a heat pump, one must account for these irreversibilities. Endoreversible thermodynamics provides an appropriate framework for this purpose, focusing on the irreversibilities occurring at the heat exchange interfaces rather than assuming perfect internal reversibility. Bădescu [6] expanded upon Jaynes' work by developing an endoreversible model to obtain a more accurate upper bound for the heating gain factor (G). By accounting for the finite-time nature of heat transfer, Bădescu demonstrated that whilst significant improvements over traditional heating remain possible—potentially reducing fuel consumption three-to-four times—the actual gains fall lower than those predicted by purely reversible models.

Building upon these foundational principles, González-Mora et al. [7] recently developed an endoreversible model specifically tailored for a photothermal Vuilleumier refrigerator. Their research explicitly links the complexities of optical solar concentration with the internal irreversibilities inherent in the thermal cycle, providing a more nuanced understanding of how external energy sources interact with the machine's internal mechanics. A key insight emerging from this work is that regenerator effectiveness (ε) exerts a dominant influence over the intensity of the energy source. Their sensitivity analysis revealed a striking disparity: the design and efficiency of the regenerator are 12 to 16 times more influential on the system's coefficient of performance (γ) than solar-specific parameters, such as concentration ratios. This finding underscores a critical pivot in the field, suggesting that the path to optimising these machines lies more in internal thermal management than in simply increasing external energy input. Furthermore, this discovery highlights a significant limitation within the existing body of literature. Most contemporary models tend to isolate their analysis, treating either the work extractor (as Bădescu's solar power models demonstrate [8,9]) or the work consumer (as Mora's refrigeration studies illustrate [7]) with a restricted focus on integrated irreversibility. Consequently, an urgent requirement exists for a unified model that simultaneously and explicitly accounts for the irreversibilities in both subunits—the work- extractor and the work-consumer. Only by integrating these components into a single analytical framework can we establish a truly comprehensive upper bound for the performance of heat-driven systems in real-world applications.

In response to the limitations identified in the existing literature, this work develops a comprehensive non-equilibrium thermodynamic model for a solar-driven heat extractor assembly. By integrating the discrete components of the thermal cycle into a single analytical framework, we aim to bridge the gap between Jaynes' idealised reversible theorems [3] and the practical constraints of real-world energy conversion.

A significant contribution of this study is the refinement and generalisation of the framework that Bădescu established [8,9]. Whilst Bădescu provided a foundational endoreversible bound, our model expands this scope by systematically isolating and eliminating specific, overly restrictive irreversibilities. This generalisation allows for broader application of the theory, providing a more versatile tool for assessing thermal systems across varying scales and operational environments.

The primary objective is to derive and evaluate rigorous performance metrics, specifically the heating gain factor (G) and the overall coefficient of performance (γ). These indicators serve as benchmarks for assessing the viability of the proposed system in capturing and upgrading solar thermal energy. Furthermore, we conduct a systematic comparison between the irreversible and endoreversible cases, illuminating how specific dissipative processes—such as finite-time heat transfer and internal friction—impact the theoretical upper bounds of efficiency. Ultimately, this analysis provides key insights essential for the future modelling of practical, Vuilleumier-type real heating machines, as previous work has done for cooling machines [7]. By quantifying the interplay between optical concentration, regenerator effectiveness, and cycle irreversibilities, we offer a robust foundation for the design and optimisation of next-generation thermal technologies.

2. Methodology

2.1. System architecture and thermodynamic configuration

We evaluate the efficiency of heating a body by considering two distinct thermodynamic scenarios, as Figure 1 schematically illustrates. Both configurations involve a thermal radiation reservoir (the Sun) at temperature

$T_{\rm H}$ and a heat sink at ambient temperature T_L. The primary objective is to quantify the rate of heat, $\dot{Q}_{\rm body}$, delivered to a body at temperature $T_{\rm b}$ (where $T_{\rm L} < T_{\rm b} < T_{\rm H}$), derived from the energy extracted from the high-temperature reservoir. A photothermal system consisting of an optical collector and an absorber facilitates this process.

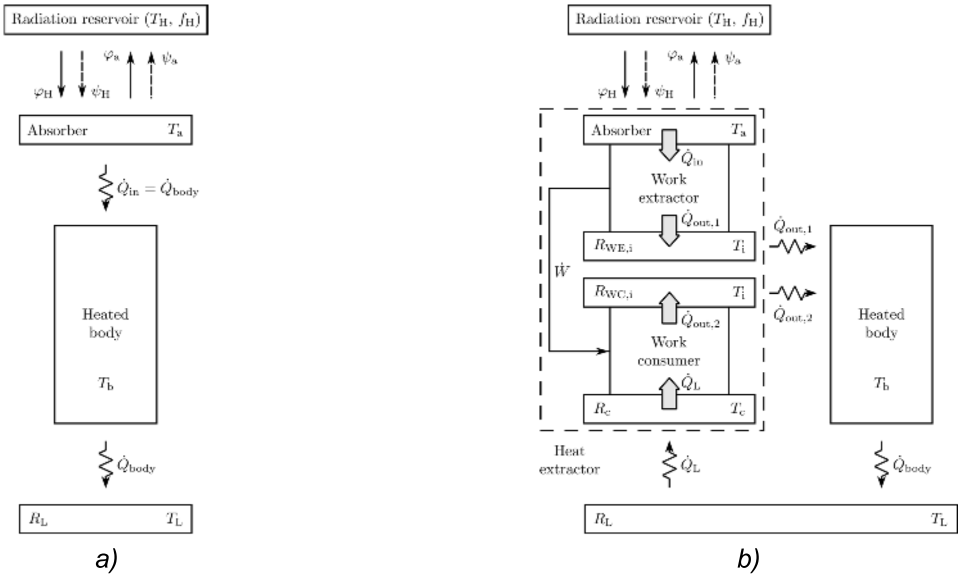

Figure. 1. *Architecture ensembles for radiative heating. a) Conventional radiation heating, b) Radiation-driven heat transformer.*

In the first configuration (Figure 1a), incident radiation from the source at $T_{\rm H}$ converts into internal energy within the collector's absorber ($\dot{Q}_{\rm a}$). Through natural dissipative processes, the heat extracted from the source degrades directly towards $T_{\rm L}$ as it traverses the system. Conversely, Figure 1b depicts what Bădescu [6] defined as the "Jaynes engine": an assembly comprising a work extractor coupled with a work consumer. In this arrangement, the work extractor redirects the power it generates entirely to drive the work consumer. Whilst Bădescu utilised the term "heat extractor" to generalise the Jaynes engine and avoid the ambiguity inherent in the term "engine" (typically associated with work extraction), we propose the more encompassing term photothermal heat transformer to describe this integrated assembly.

To establish the fundamental limits of transforming thermal radiation at $T_{\rm H}$ to heat a body at T_b, we apply the following operational assumptions to both configurations:

1. Irreversible operation of subsystems: We do not restrict the work extractor and work consumer to reversible operation. This assumption extends the model's applicability from specific Vuilleumier configurations to any thermal device sharing the architecture that Figure 1 displays.
2. Steady-state operation: The system operates under nominal conditions where thermodynamic properties represent time-averaged values, exhibiting local invariance during the measurement period.
3. Blackbody absorber characteristics: We characterise the finite-area absorber ($A_{\rm a}$) as a blackbody Lambertian radiator, capturing all incident solar radiation whilst maintaining quasi-equilibrium through thermal emission at temperature $T_{\rm a}$
4. Interfacial temperature homogeneity: We assume homogeneous temperatures at the system interfaces. This eliminates interfacial thermal gradients, ensuring unidirectional heat flow without necessitating temperature averaging—a treatment consistent with the intensive nature of temperature. Furthermore, this allows us to characterise thermal conductance and define the temperature differentials across these interfaces.
5. Photon gas dynamics: We calculate energy and entropy contributions from the radiative reservoir at $T_{\rm H}$ as undiluted and undeformed photon gas fluxes. This enables precise computation of the radiative energy rate flux density, φ_i, and radiative entropy rate flux density, ψ_i, in accordance with established Planck theory, which Eqs. (1) and (2) describe.

$$\varphi_i = \xi_i \sigma T_i^4, \quad (1)$$

$$\psi_i = \frac{4}{3}\xi_i \sigma T_i^3, \quad (2)$$

where ξ_i represents the concentration-acceptance product, Eq. (3), which considers the geometric view factor ($f_{\rm H}$) of radiation sources without chemical potential [7], and T_i denotes the temperature of the reservoir. For the specific case where the radiation reservoir corresponds to the Sun observed from Earth, this yields $f_{\mathrm{H}} = 2.166 \times 10^{-5}$. Under concentrated solar radiation conditions, the radiation reservoir's view factor scales proportionally with the concentration ratio (C_g), which depends on the concentrating technology; therefore, this formulation can include any photothermal system (with or without concentration).

$$\xi_i = C_g f_{\mathrm{H}}. \quad (3)$$

To conclude the characterisation of the system's thermodynamic performance, we establish two primary indicators. These metrics will serve as the analytical foundation for the specific configurations that we develop in the subsequent subsections. The first indicator is the heating gain factor (G), which applies to both the direct degradation and the coupled assemblies that Figure 1 illustrates. This factor quantifies the efficacy of the heating process, defining it as the ratio between the thermal power delivered to the target body ($\dot{Q}_{\mathrm{body}}$) and the heat flux that the system extracts from the high-temperature reservoir ($\dot{Q}_{\mathrm{H}}$):

$$G = \frac{\dot{Q}_{body}}{\dot{Q}_H}. \quad (4)$$

It is important to highlight that, when evaluating the integrated photothermal heat transformer (Figure 1b), we use this definition to characterise the coefficient of performance (γ). By applying this gain factor to the coupled work-extractor and work-consumer assembly, we derive a performance metric consistent with the Vuilleumier cycle modelling that González-Mora et al. [7] established, effectively representing the overall efficiency of the coupled system.

2.2. Conventional radiation heating system

Following the considerations that Section 2.1 establishes, we can establish the energy balance for the absorber in a conventional heating configuration (Figure 1a) as:

$$\dot{Q}_a = A_{\mathrm{a}}(\varphi_{\mathrm{H}} - \varphi_{\mathrm{a}}). \quad (5)$$

In this formulation, we assume the re-emission from the absorber to be diffuse and hemispherical. It is important to highlight that, within this equation, we account only for radiative losses; we neglect convective and conductive losses to the ambient environment. We make this assumption deliberately to establish the absolute upper bound of thermodynamic performance for this scenario. Applying the general definition of the gain factor (G) from Eq. 4, we obtain:

$$G = \frac{A_{\mathrm{a}}(\varphi_{\mathrm{H}} - \varphi_{\mathrm{a}})}{A_{\mathrm{a}}\varphi_{\mathrm{H}}}. \quad (6)$$

Regarding the heat transfer to the target body, the model incorporates the thermal conductance from the absorber to the body (λ_{a}), whilst also accounting for the thermal degradation resulting from the conductive coupling between the body and the ambient environment (λ_{b}):

$$\dot{Q}_{\mathrm{a}} = \dot{Q}_{\mathrm{body}} = \lambda_{\mathrm{a}}(T_{\mathrm{a}} - T_{\mathrm{b}}) = \lambda_{\mathrm{b}}(T_{\mathrm{b}} - T_{\mathrm{L}}). \quad (7)$$

Consequently, we can reformulate the absorber temperature (T_{a}) as a function of the target body temperature (T_{b}). Given that the primary objective of the process is to maintain the body at a specific thermal state, with Eq. (7), we define T_{a} as:

$$T_{\mathrm{a}} = \frac{T_{\mathrm{b}}(\lambda_{\mathrm{a}} + \lambda_{\mathrm{b}}) - \lambda_{\mathrm{b}} T_{\mathrm{L}}}{\lambda_{\mathrm{a}}}, \quad (8)$$

so we can describe the gain factor of Eq. (6) as:

$$G = 1 - \frac{1}{\xi_{\mathrm{H}}}\left[\frac{T_{\mathrm{L}}\lambda_{\mathrm{b}} - T_{\mathrm{b}}(\lambda_{\mathrm{a}} + \lambda_{\mathrm{b}})}{\lambda_{\mathrm{H}} T_{\mathrm{H}}}\right]^4. \quad (9)$$

However, a first-law analysis alone proves insufficient. We must complement this with a Second Law assessment to account for the inherent irreversibilities of the heating process. We express the entropy balance for the absorber as follows:

$$\dot{S}_{\mathrm{gen,a}} = A_{\mathrm{a}}(\psi_{\mathrm{a}} - \psi_{\mathrm{b}}) + \frac{\dot{Q}_{\mathrm{a}}}{T_{\mathrm{a}}} \geq 0. \quad (10)$$

This relation proves critical because it establishes a fundamental thermodynamic constraint on the operating temperature of the absorber. By extension, and through the substitution that Eq. (10) provides, it defines the permissible temperature range for the target body:

$$\xi_{\mathrm{H}} + \frac{1}{3}\left(\frac{T_{\mathrm{a}}}{T_{\mathrm{H}}}\right)^4 - \frac{4}{3}\xi_{\mathrm{H}}\frac{T_{\mathrm{a}}}{T_{\mathrm{H}}} \geq 0. \quad (11)$$

To conclude this analysis, we must consider the physical limits of the operational temperature. The absorber temperature, T_{a}, as Eq. (8) defines, reaches its upper bound when the photothermal system achieves thermal equilibrium, commonly referred to as the stagnation condition. As Eq. (12) demonstrates, this limit depends inherently on the specific characteristics of the employed photothermal assembly. Once the system reaches this stagnation state, the absorber cannot heat further, and entropy generation attains its theoretical minimum. However, Eq. (9) reveals that this minimum remains, in general, finite and non-zero. This indicates that the heating process preserves an inherent degree of irreversibility, which can only vanish in the idealised case of total solar concentration ($\xi_H = 1$), and consequently, the heating gain factor vanishes.

$$T_{\mathrm{a}} = T_{\mathrm{H}}\xi_{\mathrm{H}}^{1/4}. \quad (12)$$

2.3. Radiation-driven heat transformer heating system

We now analyse the configuration that Figure 1b illustrates, which operates as a radiation-driven heat transformer. This assembly comprises a work extractor integrated with a work consumer; crucially, no net work exchange occurs with the external environment. Instead, the system facilitates thermal energy interactions between the radiative source, the heat sink, and the target body. Building upon the framework for work extractors in contact with various heat reservoirs that González-Mora [10] established, we adapt these principles to the current photothermal assembly.

Within the work extractor component, the absorber captures energy from the radiative source and transfers it in its entirety to the extractor unit. As with the conventional heating scenario, we neglect convective losses to ensure the determination of the theoretical upper performance limit. Thus, we give the energy balance at the absorber as:

$$\dot{Q}_{\mathrm{a}} = A_{\mathrm{a}}(\varphi_{\mathrm{H}} - \varphi_{\mathrm{a}}) = \dot{Q}_{\mathrm{in,WE}}. \quad (13)$$

We describe the internal energy interactions within the work extractor by:

$$\dot{Q}_{\mathrm{in,WE}} - \dot{Q}_{\mathrm{out,1}} = \dot{W}_{\mathrm{WE}}, \quad (14)$$

where $\dot{Q}_{\mathrm{out,1}}$ represents the thermal power discharged to the target body and $\dot{W}_{\mathrm{WE}}$ denotes the mechanical power generated. Utilising the standard definition for work extractor efficiency, $\eta_{\mathrm{WE}} = \dot{W}_{\mathrm{WE}}/\dot{Q}_{\mathrm{in,WE}}$, we may reformulate Eq. (14) as:

$$\dot{Q}_{\mathrm{out,1}} = \dot{Q}_{\mathrm{in,WE}}(1 - \eta_{\mathrm{WE}}). \quad (15)$$

The primary function of the work consumer is to utilise the entirety of the mechanical power $\dot{W}_{\mathrm{WE}}$ to upgrade thermal energy from the ambient sink to the target body—a process we term temperature upgrading. We define the energy interactions within the work consumer as:

$$\dot{W}_{\mathrm{WE}} = \dot{Q}_{\mathrm{in,WE}} - \dot{Q}_{\mathrm{out,2}}, \quad (16)$$

where $\dot{Q}_{\mathrm{out,2}}$ represents the thermal power delivered to the target body. By incorporating the coefficient of performance ($\gamma = \dot{Q}_{\mathrm{out,2}}/\dot{W}_{\mathrm{WE}}$), we express Eq. (16) as:

$$\dot{Q}_{\mathrm{out,2}} = \gamma\dot{W}_{\mathrm{WE}} = \gamma\eta_{\mathrm{WE}}\dot{Q}_{\mathrm{in,WE}}. \quad (17)$$

Consequently, the target body receives a cumulative heat flux derived from both subunits, such that:

$$\dot{Q}_{\mathrm{body}} = \dot{Q}_{\mathrm{out,1}} + \dot{Q}_{\mathrm{out,2}} = \dot{Q}_{\mathrm{in,WE}}(1 - \eta_{\mathrm{WE}} + \gamma\eta_{\mathrm{WE}}). \quad (18)$$

For this integrated assembly, we define the heating gain factor (G’) using Eqs. (1), (4) and (18) by the following relation:

$$G' = \frac{\dot{Q}_{\mathrm{body}}}{A_{\mathrm{a}}\varphi_{\mathrm{H}}} = \left[1 - \frac{1}{\xi_{\mathrm{H}}}\left(\frac{T_{\mathrm{a}}}{T_{\mathrm{H}}}\right)^4\right](1 - \eta_{\mathrm{WE}} + \gamma\eta_{\mathrm{WE}}), \quad (19)$$

In accordance with the general characterisations that González-Mora [10] provides, we establish the efficiency of the work extractor as:

$$\eta_{\mathrm{WE}} = \left[1 - \frac{1}{\xi_{\mathrm{H}}}\left(\frac{T_{\mathrm{a}}}{T_{\mathrm{H}}}\right)^4\right]\left(1 - \frac{\lambda_{\mathrm{i}}T_{\mathrm{b}}}{\lambda_{\mathrm{i}}T_{\mathrm{a}} + A_{\mathrm{a}}(\xi_{\mathrm{H}}\sigma T_{\mathrm{H}}^4 - \sigma T_{\mathrm{a}}^4) + T_{\mathrm{a}}\dot{S}_{\mathrm{gen,WE}}}\right)$$

$$- \frac{\lambda_{\mathrm{i}}T_{\mathrm{b}}T_{\mathrm{a}}\dot{S}_{\mathrm{gen,WE}}}{A_{\mathrm{a}}\xi_{\mathrm{H}}\sigma T_{\mathrm{H}}^4(\lambda_{\mathrm{i}}T_{\mathrm{a}} + A_{\mathrm{a}}(\xi_{\mathrm{H}}\sigma T_{\mathrm{H}}^4 - \sigma T_{\mathrm{a}}^4) + T_{\mathrm{a}}\dot{S}_{\mathrm{gen,WE}})}. \quad (20)$$

Similarly, adapting this description for the coefficient of performance of the work consumer yields:

$$\gamma = \frac{1}{1-\sqrt{\frac{T_L}{T_a}\left(1-\frac{\lambda_i(T_b-T_i)}{\frac{1}{T_c}[T_b\lambda_L(T_c-T_L)+T_c\lambda_i(T_b-T_i)]}\right)}}. \quad (21)$$

Substituting Eqs. (20) and (21) allows us to determine the overall gain factor for the photothermal heat converter. Under the idealised condition where both the work extractor and work consumer operate reversibly, the efficiency of the work extractor and the coefficient of performance become:

$$\eta_{WE} = \left[1-\frac{1}{\xi_H}\left(\frac{T_a}{T_H}\right)^4\right]\left(1-\frac{\lambda_i T_b}{\lambda_i T_a + A_a(\xi_H\sigma T_H^4-\sigma T_a^4)}\right), \quad (22)$$

$$\gamma = \frac{1}{1-\sqrt{\frac{T_L}{T_b}}}. \quad (23)$$

2.4. Comparison of the heating modes

To compare the two heating modes, we define two analytical steps. The first step involves a comparative analysis of the two proposed heating architectures, which reveals a significant increase in parametric complexity when transitioning from conventional to transformer-based systems. As Eq. (9) establishes, four primary variables govern the performance of the conventional radiative heating process: the target body temperature (T_b), the thermal conductances (λ_a and λ_b), and the concentration-acceptance product (ξ_H). In contrast, the performance of the photothermal heat converter, which Eq. (19) defines, is multifaceted; it depends not only on the aforementioned parameters but also on the absorber area (A_a), the intermediate conductances (λ_i), and the internal temperatures (T_i and T_c). However, not all of these parameters remain independent, as we can easily relate them, thus reducing the number of truly independent variables.

Consequently, with eight independent variables influencing the heat transformer assembly, both Eq. (9) and Eq. (19) establish a complex multivariate functional dependence for their respective gain factors. Given the fixed boundary conditions—specifically the source temperature (T_H) and the ambient sink temperature (T_L) we must identify which of these variable parameters exerts dominant control over the gain factors across both operational scenarios.

To systematically quantify these governing influences, we employ a normalised sensitivity analysis methodology. This approach evaluates the relative sensitivity coefficient for each parameter, defining it as the proportional change in the performance—representing either metric representing either G or G'—per unit proportional change in the input variable. Formally, we express this sensitivity analysis as:

$$S_{\mu_j} = \left|\frac{\partial G}{\partial \mu_j}\frac{\mu_j}{G}\right| \text{ and } S'_{\mu_j} = \left|\frac{\partial G'}{\partial \mu_j}\frac{\mu_j}{G'}\right|. \quad (24)$$

In Eq. (24), μ_j represents each of the independent parameters that collectively define the hypersurface of the gain factors. The relative sensitivity coefficients, S_{μ_j} and S'_{μ_j}, provide a dimensionless measure of the responsiveness of G and G' to marginal variations in each independent parameter. This coefficient enables a direct, objective comparison of parameter influences across different physical dimensions and scales. We identify parameters yielding higher absolute values of S_{μ_j} as dominant control variables, which most significantly constrain system performance under specific operational conditions. By distinguishing primary from secondary influencing factors, this analytical approach rigorously prioritises optimisation efforts for future practical implementations.

For the secondary comparative analysis, we perform a direct evaluation of the relative performance between G and G'. It is noteworthy that Eq. (19), even when we assume a perfectly reversible assembly, represents a significantly more complex thermodynamic model than the conventional heating approach that Eq. (6) describes. However, a rigorous comparison of these expressions yields a fundamental result:

$$G' - G = \left[1-\frac{1}{\xi_H}\left(\frac{T_a}{T_H}\right)^4\right]\eta_{WE}(\gamma-1) > 0. \quad (25)$$

Equation (25) demonstrates that the heating gain factor which the heat transformer assembly achieves consistently exceeds that of the conventional configuration. This finding holds profound theoretical and practical interest; it remains valid regardless of the specific values of η_{WE} and γ, implying that the heat transformer maintains a superior performance limit even when we fully account for internal irreversibilities.

Furthermore, we define the ratio between these two metrics as:

$$\frac{G'}{G} = 1 + \eta_{WE}(\gamma-1) > 0, \quad (26)$$

This ratio consistently exceeds unity. This ratio serves as a critical diagnostic tool, allowing us to directly quantify the percentage improvement in heating effectiveness that the heat transformer assembly provides over conventional methods.

Finally, consistent with the framework that González-Mora et al. [7] established, we should emphasise that the gain factor G' for the heat transformer assembly is functionally equivalent to the coefficient of performance for this class of system. This alignment connects our results with the established literature on Vuilleumier-type machines [5,11], reinforcing the role of the photothermal heat converter as a high-efficiency alternative for modern thermal demand, as the literature described nearly a century ago.

3. Results and discussion

This numerical investigation evaluates the performance characteristics of a solar-driven heating process, comparing a conventional radiative heating system with the proposed radiation-driven heat transformer. As Section 2.4 establishes, the analysis focuses on the independent variables unique to each architecture to identify the primary drivers of thermodynamic efficiency. We interpret the sensitivity coefficients (S_{μ_j}) as the elasticity of the performance metric relative to its governing parameters. A value of $S_{\mu_j} = 1$ indicates a unit-proportional response (a 1% change in the variable results in a 1% change in the gain factor). Values significantly greater than unity denote high parametric sensitivity, whereas values below unity suggest that the system performance remains relatively robust against marginal fluctuations in those specific variables.

To ensure the practical relevance of this study, the analysis assumes a target body temperature of $T_\mathrm{b} = 500\ \mathrm{K}$ ($220\ °\mathrm{C}$), a value representative of numerous medium-to-high temperature industrial processes. Under these conditions, we set the concentration-acceptance product (ξ_H) at 4.33×10^{-4}, corresponding to commercially available parabolic trough collectors ($C_g \approx 20$). Furthermore, to account for optical imperfections and real-world losses, we maintain the operating absorber temperature (T_a) at 75 % of its theoretical stagnation value. Figure 2 displays these results.

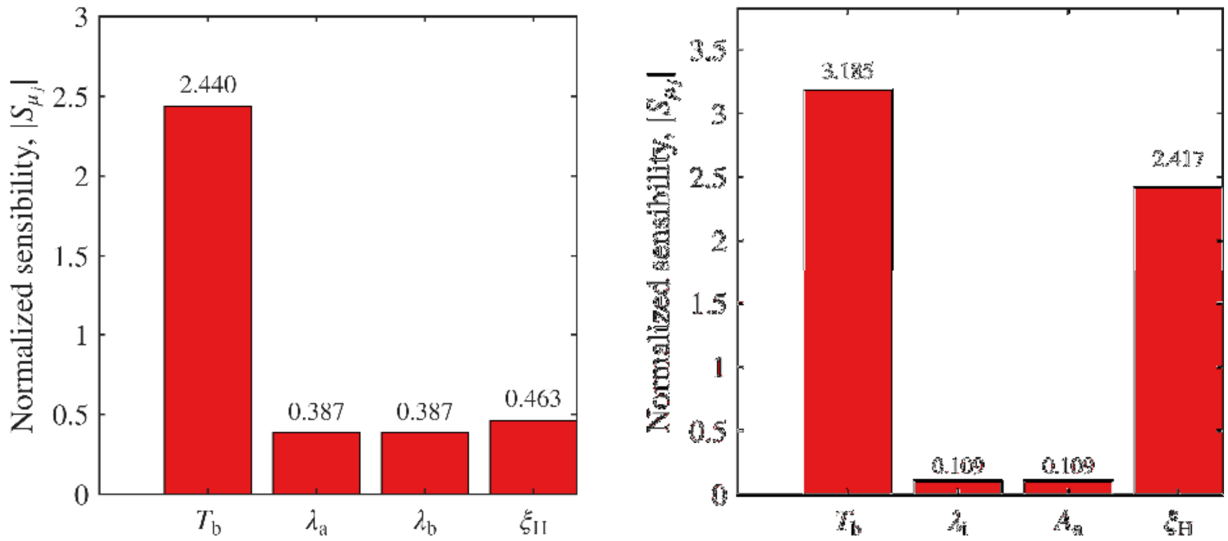

a) b)

Figure. 2. *Normalized sensibility results: a) Conventional radiation heating, b) Radiation-driven heat transformer.*

For the conventional radiative heating system, the sensitivity analysis evaluates four variables: target temperature (T_b), thermal conductances (λ_a and λ_b), and the concentration-acceptance product (ξ_H). As Figure 2a illustrates, the target body temperature (T_b) emerges as the dominant control variable, yielding a sensitivity coefficient of 2.44. This finding indicates that for every 1 % increase in the required delivery temperature, the gain factor G decreases by 2.44 %, highlighting the steep thermodynamic cost of high-grade heat in non-coupled systems. In contrast, the system displays significantly lower sensitivity to the concentration-acceptance product ($\xi_\mathrm{H} = 0.46286$) and the thermal conductances (λ_a, $\lambda_\mathrm{b} = 0.38733$). This suggests that in conventional architectures, once the system meets a certain optical threshold, performance is primarily constrained by the temeprature gradient between the source and the load rather than by the heat transfer interfaces or optical intensity.

To further elucidate these findings, a breakdown of the relative percentage contributions reveals that the target body temperature (T_b) accounts for an overwhelming 66.4 % of the total parametric influence on the gain factor. This confirms that conventional radiative heating is fundamentally "temperature-locked"; its performance depends almost exclusively on the thermal grade required by the end-use process. The concentration-acceptance product (ξ_{H}) and the thermal conductances (λ_{a}, λ_{b}) contribute more modestly, at 12.6 % and 10.5 %, respectively. From an engineering perspective, these results suggest that in a direct-degradation architecture, marginal improvements in insulation or optical precision yield diminishing returns. The intrinsic thermodynamic penalty of allowing high-grade solar radiation to degrade directly to the target temperature remains the primary bottleneck, leaving little room for optimisation through external system parameters.

The transition to the radiation-driven heat transformer (Figure 2b) reveals a more complex and responsive parametric landscape. In this scenario, T_b remains the dominant variable, but its influence amplifies notably, reaching a coefficient of 3.1847. This heightened sensitivity suggests that the coupled work-extractor and work-consumer architecture is more delicately tuned to the target thermal state, offering higher gains but requiring more precise temperature management.

Perhaps the most striking finding is the dramatic increase in the sensitivity to the solar concentration acceptance product (ξ_{H}), which rises to 2.4171—a five-fold increase compared to the conventional case. This result underscores a fundamental shift in system behaviour: whilst conventional systems remain relatively indifferent to marginal increases in concentration, the heat transformer's performance depends critically on optical quality. Conversely, the intermediate thermal conductance (λ_{i}) and the absorber area (A_{a}) exert minimal influence ($S_{\mu_j} = 0.10939$), indicating that the assembly's efficiency is limited by its thermodynamic coupling and optical input rather than its internal mechanical dimensions.

These results demonstrate that whilst conventional heating is primarily limited by the 'thermal distance' to the target, the heat transformer acts as an 'optical leverage' system, where enhancements in solar concentration translate much more effectively into heating gains.

In the heat transformer assembly, the distribution of parametric influence undergoes a profound structural shift, transitioning towards an optical-intensive regime. Whilst the target temperature (T_{b}) remains the primary factor at 54.7 %, its dominance tempers noticeably due to the surging importance of the concentration acceptance product (ξ_{H}), which now accounts for 41.5 % of the system's sensitivity. This near-parity between delivery temperature and optical input indicates that the heat transformer effectively acts as a thermodynamic multiplier, where the quality of the incoming radiation leverages far more efficiently to overcome thermal gradients. Conversely, the internal geometric and transport parameters—specifically the intermediate thermal conductance (λ_{i}) and the absorber area (A_{a})—show a marginal contribution of only 1.9 % each. This finding implies that once the heat transformer architecture is established, the design focus should pivot decisively towards high-precision optical concentration rather than internal mechanical resizing, as the system's superior performance is sustained by the synergy between high-source quality and work-coupled heat upgrading.

To establish the ultimate potential of both configurations, we evaluate their performance within the endoreversible limit. In this regime, we neglect internal irreversibilities, focusing exclusively on the unavoidable dissipative processes at the heat transfer interfaces. By assuming idealised thermal conductances, we can identify the maximum attainable values for G and G' across a spectrum of solar concentration technologies, as characterised by varying values of ξ_H.

The numerical evaluation, which Figure 3 illustrates, utilises the boundary conditions of $T_{\mathrm{L}} = 293.15\ \mathrm{K}$ and $T_{\mathrm{H}} = 5777\ \mathrm{K}$. We vary the absorber temperature (T_{a}) between the ambient sink (T_{L}) and its stagnation limit ($T_{\mathrm{a,max}}$), which Eq. (12) defines. In the resulting plot, solid lines denote the conventional radiation heating system, whilst marked lines represent the radiation-driven heat transformer.

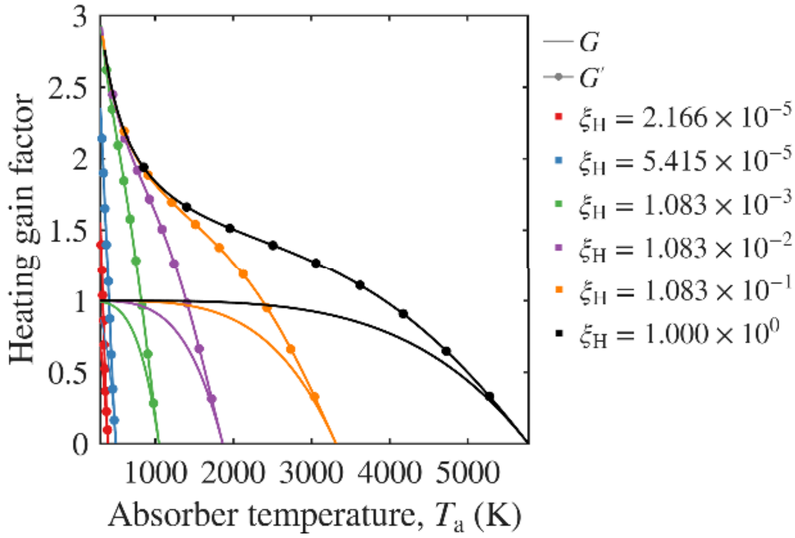

Figure. 3. *Heat gain factor for the radiative heating process.*

For the conventional configuration, the results align strictly with the constraints of Eq. (6). The maximum achievable heating gain factor (G) is fundamentally capped at unity. Physically, this represents the limit where solar energy converts entirely into heat without any work-enhanced upgrading. A notable feature of these curves is their exceptionally steep negative slope; the gain factor diminishes rapidly as the target temperature increases. Whilst high-concentration technologies ($\xi_{\mathrm{H}} \to 1$) provide a slightly more stable profile, the system remains severely constrained by the direct degradation of high-grade radiation.

In contrast, the radiation-driven heat transformer consistently demonstrates the superiority that Eqs. (25) and (26) predict, with $G' > G$ across the entire operational range. Unlike the conventional case, this assembly leverages the thermodynamic potential of the source to achieve gain factors significantly greater than one—a feat impossible for direct heating systems.

A compelling phenomenon emerges in systems with high geometric concentration: as T_{a} increases, the curves exhibit a distinct inflection point or "stability zone." In this region, the slope of the gain factor levels off momentarily, indicating a range where the work-coupling mechanism effectively compensates for increasing thermal gradients. Eventually, however, the unyielding laws of radiative physics prevail; as T_{a} continues to rise, the T^4 dependence of radiative losses to the environment causes an inevitable decline in the gain factor.

The observed decay of the gain factor with increasing absorber temperature is an expected consequence of the heightened radiative exchange with the surroundings. However, this creates a classic thermodynamic trade-off: whilst higher absorber temperatures increase entropy production and radiative losses, they also expand the available work potential (exergy) of the system. The heat transformer is uniquely capable of harvesting this potential, ensuring that even as the curves decline, the thermal leverage that the integrated work extractor/consumer assembly provides remains vastly more efficient than conventional methods.

4. Conclusions

This study developed a comprehensive non-equilibrium thermodynamic model for a solar-driven heat extractor assembly, comprising an irreversible radiative work extractor coupled with an irreversible work consumer. By systematically incorporating irreversibilities from both external heat transfer—radiative and conductive—and internal dissipation, we established a generalised framework for analysing photothermal heat transformers. From this general case, we derived the endoreversible condition by relaxing internal irreversibility assumptions, thereby isolating the performance limit imposed solely by external heat exchange constraints.

We demonstrated that the radiation-driven heat transformer consistently outperforms conventional radiative heating across all operational regimes, achieving gain factors significantly greater than unity—a feat fundamentally impossible for direct degradation systems. The analysis revealed a ~~profound~~ likely structural shift in parametric influence when transitioning to the coupled architecture: the sensitivity to solar concentration ratio increases five-fold, attaining near-parity with target temperature as a dominant control variable. Specifically, the target temperature accounts for 54.7 % of total parametric influence in the transformer, whilst optical concentration contributes 41.5 %, compared to 66.4 % and 12.6 %, respectively, in conventional systems. Furthermore, the endoreversible analysis confirmed that, whilst both configurations ultimately decline with increasing absorber temperature due to radiative losses, the transformer maintains superior performance across the entire operational envelope.

By deliberately neglecting convective and conductive losses to establish absolute upper bounds, this work necessarily omits certain real-world dissipative mechanisms that would further constrain performance in practical implementations. Additionally, the analysis assumes idealised internal coupling between work extractor and work consumer, which in practice would be limited by regenerator effectiveness—a factor that recent investigations of analogous Vuilleumier-type systems have highlighted as critically influential. These idealisations imply that the reported gain factors represent true thermodynamic upper bounds rather than achievable performance levels, and designers should interpret them as optimisation targets rather than operational expectations.

The findings significantly refine and extend the foundational bounds that previous endoreversible models established, demonstrating that the performance limits for photothermal heating are substantially more nuanced than previously recognised. By explicitly modelling irreversibilities in both subsystems, we reveal that optical concentration assumes a role of unprecedented importance in coupled architectures—an insight absent from earlier work that treated either the work extractor or consumer in isolation. This investigation also bridges the idealised reversible theorems of the mid-twentieth century with the practical engineering developments that preceded them, whilst establishing a unified analytical framework that encompasses both heating and cooling applications.

Future investigations should focus on incorporating finite regenerator effectiveness into the current irreversible framework, as sensitivity analyses from both this study and prior cooling research identify this component as critically limiting. Exploring transient operational behaviour under variable solar irradiation would provide valuable insights for practical system design, as would the inclusion of convective and conductive losses to establish more realistic performance bounds. Extending the analysis to optimise the trade-off between absorber temperature, exergy capture, and radiative losses also warrants further investigation.

This work establishes a rigorous thermodynamic benchmark for solar-driven heat amplification, providing engineers and system designers with fundamental performance limits against which to evaluate real-world components—absorbers, heat exchangers, and regenerators. By quantifying the interplay between optical concentration and thermodynamic coupling, the findings inform the rational design of next-generation solar thermal technologies aimed at decarbonising industrial process heat, offering a pathway to significantly reduce primary energy consumption in the heating sector—a critical step towards global energy sustainability.

Acknowledgments

The authors appreciate the support provided by COMECyT through the program 'Investigadoras e Investigadores COMECyT' to EGM. This work, conducted as part of the AESCo project, was made possible by the resources and funding granted under this initiative.

Nomenclature

Example:

A area, m^2

C concentration ratio

f geometric view factor

G heating gain factor

$\dot{Q}$ heat transfer rate, W

S relative sensitivity coefficient

$\dot{S}$ entropy rate, W/K

T temperature, K

Greek symbols

γ coefficient of performance

η efficiency

λ thermal conductance, W/K

μ independent parameter, W/K

ξ concentration acceptance product

σ Stefan-Boltzmann constant

φ energy rate flux density, W/m^2

ψ entropy rate flux density, $W/m^2 \cdot K$

Subscripts and superscripts

a absorber

b body

gen generation

i counter

in input

j counter

L low temperature reservoir

H high temperature radiation reservoir

out out

WE work extractor

References

[1] REN21. Renewables 2025 Global Status Report Collection, Global Overview. Paris: 2025.

[2] Müller I. A History of Thermodynamics. Berlin, Heidelberg: Springer Berlin Heidelberg; 2007. https://doi.org/10.1007/978-3-540-46227-9.

[3] Jaynes ET. Note on thermal heating efficiency. Am J Phys 2003;71:180–2. https://doi.org/10.1119/1.1508446.

[4] Vuilleumier R. Method and apparatus for inducing heat changes 1918.

[5] Wurm J, Kinast JA, Roose TR, Staats WR. Stirling and Vuilleumier Heat Pumps: Design and Applications. 1st ed. McGraw-Hill; 1991.

[6] Bădescu V. Accurate upper bound for heating gain factor. Europhysics Letters (EPL) 2006;76:568–74. https://doi.org/10.1209/epl/i2006-10318-y.

[7] González-Mora E, Poudel R, Durán-García MD. Endoreversible description of photothermal Vuilleumier refrigeration machines. Journal of Non-Equilibrium Thermodynamics 2026;51:103–14. https://doi.org/10.1515/jnet-2025-0094.

[8] Bădescu V. Note on the maximum photothermal heating efficiency. Journal of Renewable and Sustainable Energy 2025;17. https://doi.org/10.1063/5.0243235.

[9] Bădescu V. Broadband approach for the most energy efficient way of radiation-driven heating. J Appl Phys 2026;139. https://doi.org/10.1063/5.0304660.

[10] González-Mora E. A framework for teaching the efficiency of realistic work extractors from thermal reservoirs. Eur J Phys 2026;47:015103. https://doi.org/10.1088/1361-6404/ae22aa.

[11] Dogkas G, Rogdakis E. A review on Vuilleumier machines. Thermal Science and Engineering Progress 2018;8:340–54. https://doi.org/10.1016/j.tsep.2018.09.004.